Adaptive simulations of cavity-based detonation in supersonic hydrogen-oxygen mixture

Xiaodong Cai[1], Jianhan Liang[1*], Ralf Deiterding[2], Zhiyong Lin[1]

[1]Science and Technology on Scramjet Laboratory

National University of Defense Technology, Changsha, 410073, China

[2]Aerodynamics and Flight Mechanics Research Group, University of Southampton

Highfield Campus, Southampton SO17 1BJ, United Kingdom

Abstract: Two-dimensional reactive Euler equations with a detailed reaction model where the molar ratio of the combustible mixture $H_2/O_2/Ar$ is 2:1:7 under the condition of pressure 6.67 kPa and temperature 298 K, are solved numerically with adaptive mesh refinement method to investigate detonation combustion using a hot jet initiation in cavity-based channels filled with the supersonic combustible mixture. Results show that from the comparison between the simulations in a cavity-based channel and a straight channel without any cavity embedded, it is indicated that the cavity can help realize detonation initiation in the combustible mixture with a hot jet. It is suggested that detonation initiation can be realized using a relatively weaker hot jet in cavity-based channels filled with the supersonic combustible mixture compared with that in straight channels without a cavity embedded. The cavity also plays a significant role in detonation propagation in the supersonic combustible mixture. After the hot jet is shut down, the acoustic wave generated by the subsonic combustion in the cavity can accelerate detonation propagation through a subsonic

Corresponding author. Email addresses: cai-chonger@hotmail.com, jhleon@vip.sina.com, r.deiterding@soton.ac.uk, linzy96@nudt.edu.cn,

channel and result in the formation of a slightly overdriven detonation eventually. For a given flow with a shadow cavity embedded, there should exist a minimum cavity width L_{min}. When the width is below L_{min}, only some pressure oscillations in the cavity can make some impacts on detonation initiation and propagation. Otherwise, cavity oscillations can be generated which can greatly accelerate detonation initiation and propagation in the supersonic combustible mixture. For the shadow cavity, purely increasing the cavity depth does not have any more influence on detonation combustion. However, if the cavity is a deep one, it can play an important role in accelerating detonation initiation and propagation in the supersonic combustible mixture due to resonant oscillations.

Key words: hydrogen-oxygen detonation, hot jet initiation, supersonic combustible mixture, cavity-based channel, adaptive mesh refinement

1 Introduction

Detonation combustion is an extremely effective method which can burn combustible mixtures and release chemical energy efficiently. The idealized thermodynamic efficiencies of constant pressure, constant volume, and detonation are 27%, 47%, and 49%, respectively[1]. Due to the inherent theoretical advantage of detonation over deflagration, investigations on detonation based engines have been promoted significantly[2-4].

The development of reliable initiation method is always one of the most important issues for detonation combustion. Direct initiation[5-7] can ignite detonation

quickly, but it is not actually applicable due to its necessary usage of large energy. An alternative approach is the utilization of a hot jet which can also ignite detonation initiation very fast[8], because the flame acceleration process of deflagration to detonation transition (DDT) is bypassed essentially. The hot jet initiation has been investigated comprehensively in quiescent combustible mixtures[9-12], but in supersonic combustible mixtures only a few experimental researches have been carried out[13-15]. Ishii et al.[13] conducted experiments in combustible mixtures whose Mach numbers were 0.9 and 1.2 to investigate detonations using a hot jet initiation. Han et al.[14][15] studied detonation initiation and DDT process using a hot jet experimentally in supersonic hydrogen-air mixtures with Mach numbers 3 and 4, where detonations were initiated through shocks or shock reflections[16-20] on the walls induced by the hot jet. A series of simulations on detonation combustion in straight channels with a hot jet initiation in supersonic hydrogen-oxygen mixtures were conducted by Cai et al.[21-25] and Liang et al.[26], where the SAMR (Structured Adaptive Mesh Refinement) framework[27] based open-source program AMROC[28-32] (Adaptive Mesh Refinement Object-oriented C++) is utilized. These numerical simulations solved the two-dimensional and three-dimensional reactive Euler equations and applied a classical second-order accurate MUSCL-TVD (Monotone Upstream-centered Schemes for Conservation Laws-Total Variation Diminishing) scheme with both a simplified reaction model[29] and a detailed reaction model[33]. It was shown by these results that for a given hot jet and flow condition there exists a critical hot jet width below which detonation initiation cannot be realized and when

the hot jet is shut down no other methods can be utilized for the control of detonation propagation. It is indicated that it is difficult to realize detonation initiation purely using a hot jet and stabilization control of detonation propagation in straight channels. Therefore, some other approaches might be needed to be cooperated together for a better configuration.

Currently, cavities are widely investigated on the feedback mechanism[34-36], especially they have been successfully used as flameholders in supersonic combustors due to their outstanding potential to stabilize combustion by cavity oscillations[37-40]. However, they have not been tried so far associated with detonation combustion in supersonic combustible mixtures. To investigate the potential usage of cavities on detonation initiation and propagation, high-resolution simulations are conducted in cavity-based channels filled with supersonic combustible mixtures using the adaptive mesh refinement method.

The remainder of this paper is organized as follows: the computational setup is presented in Section 2, including the introduction of the computational model and numerical scheme. A convergence analysis is discussed in Section 3. Results of the simulations are shown in Section 4, in which cavity-based detonation initiation and propagation, and effects of different cavity sizes including the width and depth, are investigated. Finally Section 5 concludes the paper.

2 Computational model

2.1 Computational setup

The simplified schematic for the calculation model is depicted in Fig.1. Reflecting boundary with slip wall conditions are used on the upper and lower wall. A small inflow which models a hot jet, is embedded into the lower wall boundary. A cavity is located downstream in the hot jet. Numerical simulations and experimental observations[41-44] indicate the existence of two types of detonation structures which are usually classified as regular (weakly unstable) and irregular (highly unstable) detonations based on the regularity of cellular structure[45-52]. Self-sustaining CJ (Chapman-Jouguet) detonations for hydrogen-oxygen mixtures highly diluted with argon in low pressure are ideal candidates for detonation simulations, because very regular cellular detonations can be generated[53], which are relatively beneficial for investigations of cavity-based detonations. The cavity-based channel consists of a stoichiometric $H_2/O_2/Ar$ mixture with a molar ratio 2:1:7 under the condition of pressure 6.67 kPa and temperature 298 K. The mixture is flowing in the channel at the CJ velocity (the referenced $V_{CJ} = 1627\ \mathrm{m/s}$). The right boundary models the inflow condition and the ideal outflow condition is imposed on the left one.

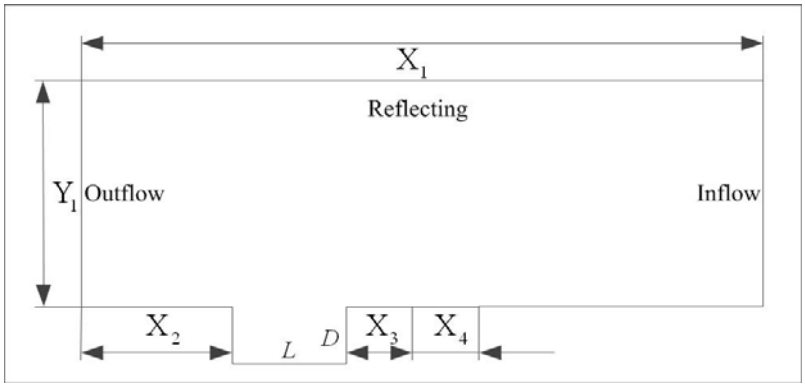

Fig.1 The schematic of the calculation model.

The hot jet is set to the equilibrium CJ state of H_2/O_2 with a stoichiometric molar ratio under the condition of pressure 6.67 kPa and temperature 298 K. This

equilibrium CJ state is calculated with Cantera[54], as shown in Table 1.

Table 1 Equilibrium CJ state for the hot jet. Note that the parameters for the nine species are given by the mass fractions.

State parameter	Value	Unit
Pressure	113585.12	Pa
Temperature	3204.8374	K
Density	0.05959	kg/m^3
Velocity	1229.9015	m/s
Energy	83445.813	J/m^3
H_2	0.024258141648492	
H	0.007952664033931	
O	0.055139351559790	
O_2	0.124622185271180	
OH	0.161144120322560	
H_2O	0.626759466258162	
HO_2	0.000117215557650	
H_2O_2	0.000006855348235	
Ar	0	

2.2 Numerical scheme

The two-dimensional reactive compressible flow utilizes the Euler equations with the detailed reaction model[33] as governing equations. The second-order accurate MUSCL (Monotone Upstream-centered Schemes for Conservation Laws)-TVD finite volume method (FVM) is used for the convective flux discretization. The hydrodynamic solution is separated into the flux calculation step and reconstruction step. Rather than Strang splitting, Godunov splitting is adopted here due to almost the same performance with Strang splitting but more computationally efficient[28]. A hybrid Roe-HLL[28] Riemann solver is used for the construction of the inter-cell

numerical upwind fluxes, while the Van Albada limiter is applied with the MUSCL reconstruction to construct a second-order method in space. As for time integration, the second-order accurate MUSCL-Hancock technique[55] is adopted. Under the condition of CFL (Courant-Friedrichs-Lewy) number 0.95, the dynamic time step is used for all the simulations.

Difference between viscous and inviscid detonations is an interesting point. Numerical diffusion is determined by grid resolution[56]. It is also demonstrated that reliability of results increases on increasing grid resolution and scheme accuracy[57]. At low grid resolution numerical diffusion dominates over physical diffusion while at high gird resolution physical diffusion dominates over numerical diffusion. Due to low numerical diffusion and absence of physical diffusion in high-resolution inviscid simulations, some small-scale unphysical features can be generated. A detailed discussion of this issue has been provided by Samtaney and Pullin[58]. However, it is observed that even in high-resolution simulations, results of inviscid and viscous detonations are qualitatively similar, especially for regular detonations. It was reported previously that similar structures of regular detonations using both Euler and Navier-Stokes (NS) equations are observed, which indicates that small-scale structures that are eliminated in inviscid simulations do not affect the overall features of regular detonations[59]. Very recent investigations have indicated that although diffusion effect is important for the evolution of irregular detonations[60-63], it does not play any role in regular detonations owing to the absence of hydrodynamic instabilities[64-66]. Therefore, the results obtained in this paper where the reactive Euler

equations are used for regular detonations are nevertheless expected to give at least qualitatively correct conclusions.

3 Verification of adaptive mesh refinement

As shown in Fig.1, the length and height of the channel are X_1 = 10 cm and Y_1 = 3 cm. The detonation cell size under the given condition is λ = 3.0 cm, so one whole detonation cell can be developed in the Y direction for this setup. The distance between the left edge of the cavity and the outflow boundary is X_2 = 3 cm. The width of the hot jet is X_4 = 0.3 cm, and the hot jet is X_3 = 0.4 cm away from the right edge of the cavity. The width and depth of the cavity are L = 2 cm and D = 1 cm. The initial mesh is 800×320. Based on previous experiments[67], a division between shadow and deep cavities is $L/D \cong 1$. When $L/D > 1$, the cavities may be considered shallow while when $L/D < 1$, the cavities may be considered deep. Therefore, the initial cavity can be considered as a shadow one. Calculated by Cantera, the induction length of one-dimensional ZND (Zel'dovich-von Neumann-Döring) model under the condition is l_{ig} = 1.509 mm. The calculations are all conducted parallel on a cluster using 72 Intel Xeon X5675-3.06 GHz processors.

For the detailed reaction model used here, a minimal $6\ Pts/l_{ig}$ spatial resolution is suggested for the one-dimensional ZND solution to resolve accurately all the intermediate reaction products[68]. However, in multi-dimensional detonations a higher resolution is required for the complete capture of internal wave structure around triple points. For regularly oscillating detonations, an effective resolution up to

44.8 Pts/l_{ig} is used in previous two-dimensional verification simulations, which indicate that this resolution is sufficient for resolving reliably even the secondary triple points[27].

However, problem-dependent thresholds for triggering adaptation based on scaled gradients of density, temperature, pressure and mass fractions of species, are needed for effective adaptive mesh refinement. As a whole, the combination of these adaption flag parameters can improve the reliability and efficiency of the mesh adaptation. Here, the threshold values on density, temperature, pressure and mass fractions of $\varepsilon_\rho = 0.5$, $\varepsilon_T = 5\times10^5$, $\varepsilon_p = 5\times10^6$, $\varepsilon_{O_2} = 4\times10^{-4}$, $\varepsilon_{H_2O} = 2\times10^{-4}$, $\varepsilon_H = 1\times10^{-3}$, $\varepsilon_O = 1\times10^{-3}$, $\varepsilon_{OH} = 1\times10^{-3}$, $\varepsilon_{H_2} = 4\times10^{-4}$ are provided, where ε represents the scaled gradient of these quantities.

Three different distributions of mesh refinement are depicted in Fig.2, where the highest resolution is 48.4 Pts/l_{ig} in Fig.2(a), 96.8 Pts/l_{ig} in Fig.2(b) and 193.6 Pts/l_{ig} in Fig.2(c), respectively. Overall, the same pattern of Mach reflection on the upper wall, slip line directly behind the triple point, bow shock induced by the hot jet, shock-induced combustion and subsonic combustion in the cavity is all observed in the three distributions, and these structures are all resolved with the highest levels (shown by the red color). Interactions of different refinement levels could create artificial numerical disturbances, so it is very important for the setting of refinement thresholds to enable adequate coverage of shock wave, combustion zone and their surrounding regions in detonation simulations. Fig.2(a)-(c) show almost the same structures and all satisfy the requirements of adequate coverage. Eventually, as a

compromise of numerical resolution and computational cost, the second highest resolution of four-level refinement with refinement factors $r_1 = 2, r_2 = 2, r_3 = 2$ in Fig.2(b) is chosen as the configuration for all the following simulations. The refinement factor is the ratio between the spatial steps Δx_l and Δx_{l-1} of levels l and $l-1$, respectively, i.e. $r_l = \Delta x_{l-1} / \Delta x_l$.

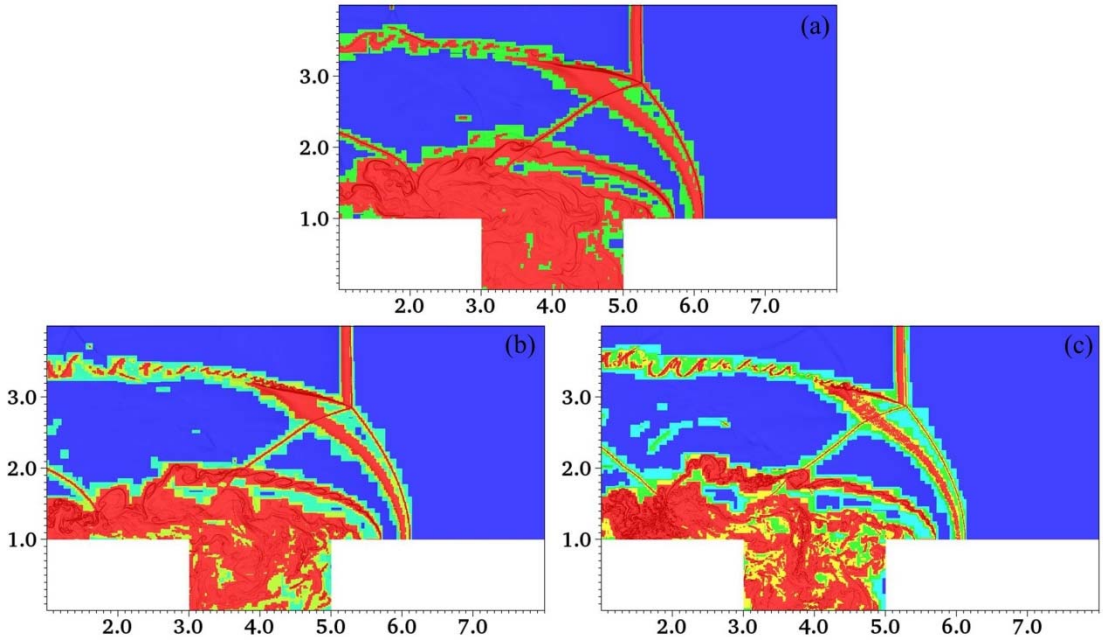

Fig.2 Distributions of three different kinds of mesh refinement: (a) three-level refinement of $r_1 = 2, r_2 = 2$; (b) four-level refinement of $r_1 = 2, r_2 = 2, r_3 = 2$; (c) five-level refinement of $r_1 = 2, r_2 = 2, r_3 = 2, r_4 = 2$.

4 Results and analysis

4.1 Cavity-based initiation

Fig.3 shows the initiation process in the supersonic combustible mixture using the hot jet in the cavity-based channel. The time interval of the four successive frames is the same, denoted $\Delta t = 61.6\ \mu s$. After the hot jet injection into the channel, a

strong bow shock is induced, as shown in Fig.3(a). The combustion front and induced shock are separated with an obvious distance, indicating that detonation initiation is not achieved at this moment. This shock wave becomes gradually stronger, but it is not strong enough to realize direct initiation. Subsequently, because of the confinement of the channel height a shock reflection is generated on the upper wall, as shown in Fig.3(b). With the increasing of the reflected shock strength, a Mach reflection is created near the upper wall with a slip line following behind, as shown in Fig.3(c). After crossing through the Mach stem, pressure and temperature of the combustible mixture are increased enough that a local Mach detonation is induced finally. This Mach detonation has propagated obviously toward the incoming flow with a velocity of V_{CJ} compared with that in Fig.3(a), which indicates that it is actually an overdriven detonation. The triple-wave point propagates along with the bow shock and is going to reflect on the lower wall, as shown in Fig.3(d), which can release more chemical energy immediately as an ignition source to sustain the continuous propagation of overdriven detonation.

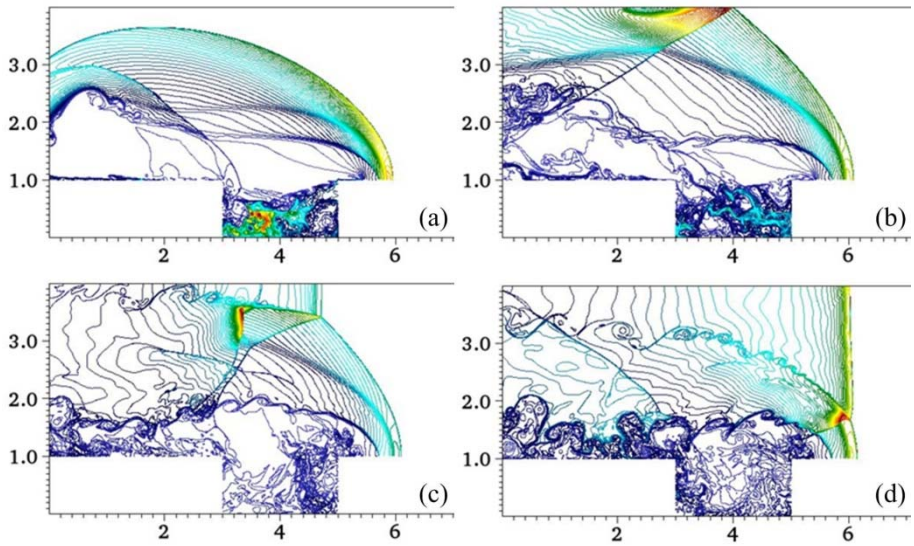

Fig.3 Density isolines showing the initiation process in a cavity-based channel. (a) $t = 229.6\ \mu s$; (b) $t = 287.43\ \mu s$; (c) $t = 348.69\ \mu s$; (d) $t = 414.37\ \mu s$.

However, simply through the process presented in Fig.3, it seems that the cavity does not play any particular role in detonation initiation in the supersonic combustible mixture. Therefore, a similar setup is conducted for comparison, which uses almost the same condition except for the only difference that the straight channel is not cavity embedded.

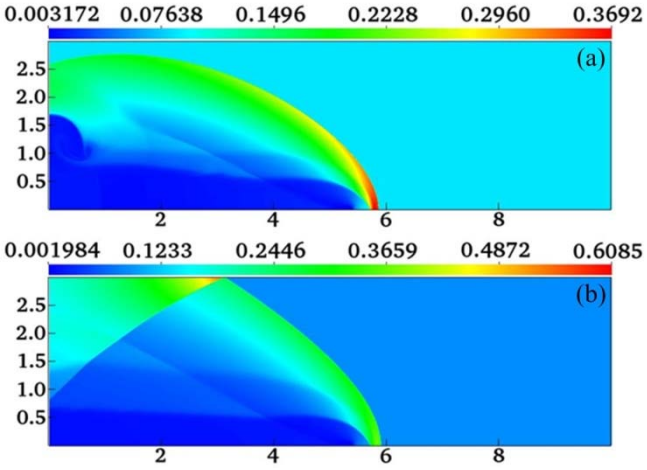

Fig.4 The hot jet induced bow shock reflection in the straight channel without the cavity embedded. The density unit of the contours is kg/m^3. (a) $t = 229.6\ \mu s$; (b) $t = 414.37\ \mu s$.

As shown in Fig.4(a), when the hot jet is injected into the supersonic combustible mixture in the straight channel, an induced bow shock is generated and subsequently a shock reflection is formed, as shown in Fig.4(b), which are similar with that in Fig.3(a)(b). However, the shock reflection structure is almost kept the same, and no further Mach reflection is generated. It could be indicated that the flow field finally maintains a dynamically stable state as the jet-induced shock reflection, but not the successful detonation initiation, which is in good agreement with Ref.

[23].

The same hot jet can initiate detonation successfully in the supersonic combustible mixture when a cavity is embedded in the channel, but it fails to realize detonation initiation in the same straight channel without the cavity embedded. Through this comparison, it is suggested that a cavity in the straight channel surely has a positive effect on detonation initiation in supersonic combustible mixtures using a hot jet initiation.

It is well known that the basic idea of using a cavity in scramjet combustors is to create a low-speed recirculation region in supersonic combustible mixtures, where flameholding may be achieved by partial subsonic combustion within the recirculation flow because a stable flame existing in the cavity can act as an ignition source continuously for the whole flow[36-40].

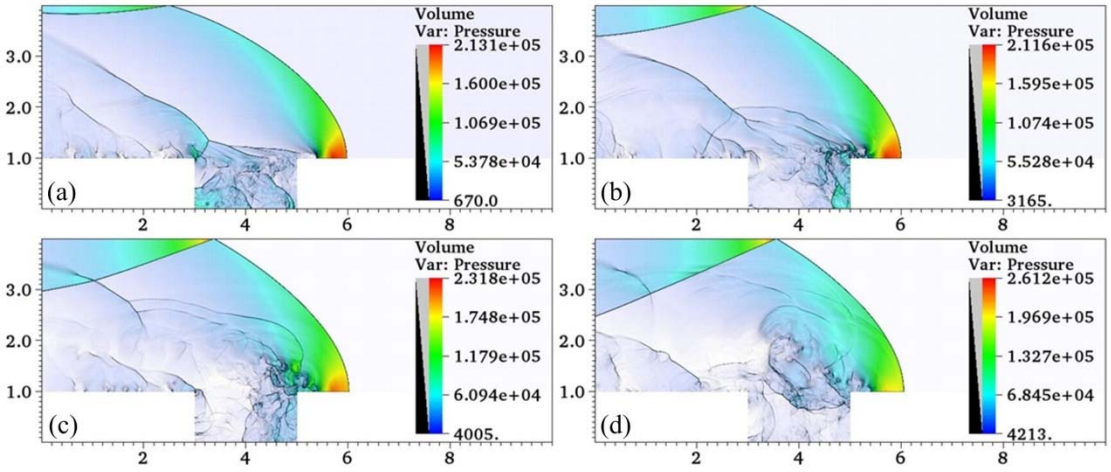

Fig.5 Pressure volume contours cooperated with schlieren images showing pressure oscillations in the cavity. The pressure unit is Pa. (a) $t = 239.11\ \mu s$; (b) $t = 247.73\ \mu s$; (c) $t = 257.2\ \mu s$; (d) $t = 267.03\ \mu s$.

As shown in Fig.5, the subsonic combustion within the cavity can result in pressure oscillations, which can help to accelerate the hot jet initiation. First in

Fig.5(a), a pressure wave is generated above the cavity. Due to cavity oscillations, the pressure wave is gradually lifted up and getting close to the front of the bow shock, as shown in Fig.5(b)(c). Eventually the pressure wave catches up with the bow shock front in Fig.5(d). It is also observed that the bow shock is lifted up at the same time owing to the pressure wave lifting up, and the pressure directly behind the bow shock becomes approximately 30% larger than that in Fig.5(a), which indicates the strength of the bow shock is enhanced along with pressure oscillations. When the bow shock reaches the critical strength after periodical pressure oscillations in the cavity, the induced detonation initiation can be realized eventually.

When the distance between the hot jet and the right edge of the cavity is increased from X_3 = 0.4 cm to X_3 = 0.8 cm, detonation initiation is also realized successfully, as shown in Fig.6. However, in Fig.6(b) it takes about $t = 467.77\ \mu s$ when the triple point is going to reflect on the lower wall while in Fig.3(d) the time is only $t = 414.373\ \mu s$ which is about $55\ \mu s$ faster than that in Fig.6(b). It is indicated that detonation initiation can be realized more quickly when the hot jet is closer to the cavity. When the distance is increased, it has to take a longer time for pressure oscillations resulted from the cavity to catch up with the bow shock, thus making detonation initiation slower.

It has been reported that cavities can help realize detonation initiation through the DDT mechanism, and an increase in the number of cavities promotes DDT as long as the flame velocity leaving the last cavity does not exceed the sonic velocity[69][70]. Once a detonation is realized through the DDT mechanism the propagation of

compression waves generated in the cavities can no longer have an influence on the detonation front. This is exactly true in quiescent combustible mixtures. However, in supersonic combustible mixtures, pressure oscillations in the cavities should still be able to play a role in the evolution of the detonation front due to the existence of the subsonic flowfield behind the detonation front.

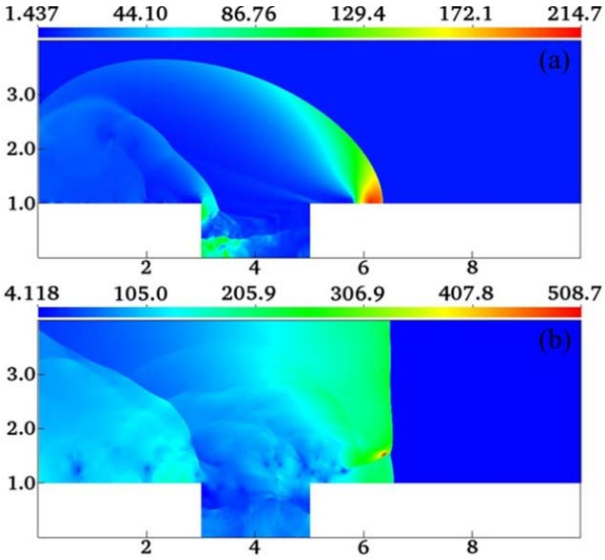

Fig.6 Pressure contours showing the successful initiation in the cavity-based channel when X_3 is increased from 0.4 cm to 0.8 cm. The pressure unit is kPa. (a) $t = 229.8\ \mu s$; (b) $t = 467.77\ \mu s$.

It is suggested by the results above that pressure oscillations produced by subsonic combustion in the cavity can help realize detonation initiation when using a hot jet. Therefore, detonation initiation can be realized successfully using a less strong hot jet in supersonic combustible mixtures when a cavity is embedded in the channel compared with that in the straight channel without a cavity embedded. During the development of propulsion systems based on detonation combustion, reliable initiation method is always a crucial issue[71]. Therefore, detonation initiation using a

hot jet with the help of a cavity embedded in the channel filled with supersonic combustible mixtures might be a newly promising approach.

4.2 Cavity-based propagation

Fig.7 shows the detonation structures in the cavity-based channel after the successful initiation. For the specified combustible mixture in the channel, the cell size of CJ detonation is $\lambda \cong 3.0\,\mathrm{cm}$. However, there appears almost three small detonation cells in the channel after the successful initiation due to the instability of overdriven detonation.

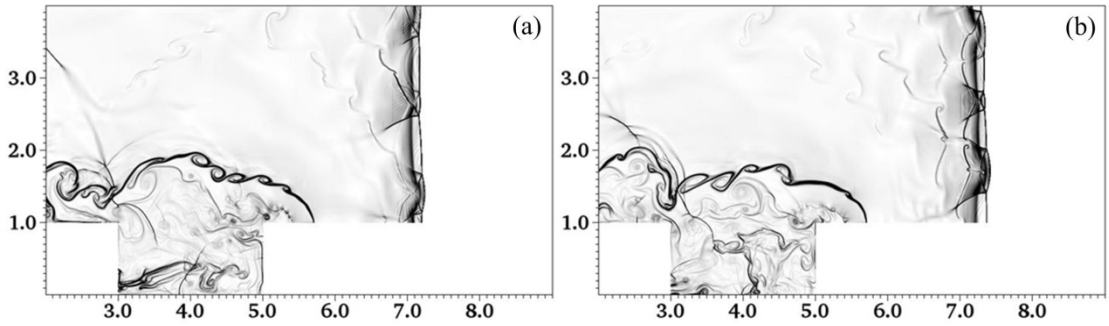

Fig.7 Density numerical schlieren images showing overdriven detonation propagation. (a) $t = 483.49\,\mu\mathrm{s}$; (b) $t = 496.11\,\mu\mathrm{s}$.

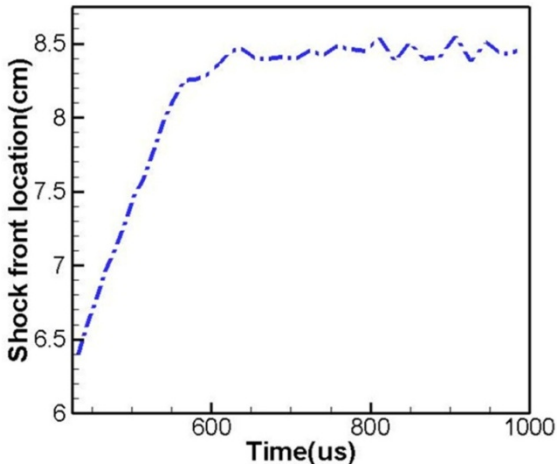

Fig.8 The location history of detonation front in the cavity-based channel. The hot jet is shut

down at $t = 500\ \mu s$.

Fig.8 records the location history of detonation front before and after the shutdown of the hot jet. The slope of the curve represents the relative propagation velocity. It is calculated that the relative propagation velocity before the shutdown of the hot jet is $v = 17.86\ m/s$, which means that the absolute propagation velocity of overdriven detonation is $V = v + V_{CJ} = 1644.86\ m/s$.

When the hot jet is shut down at $t = 500\ \mu s$, overdriven detonation gradually attenuates and becomes weaker without the help of the hot jet[21]. One of the characteristics is that the propagation velocity gradually decreases. As shown in Fig.8, after about $t = 800\ \mu s$ the curve approximately becomes an aclinic line which suggests that detonation wave basically is kept in the same location along with minor oscillations. Therefore, the relative propagation velocity is obtained as almost $v_1 = 0$, and the absolute propagation velocity is $V_1 = v_1 + V_{CJ} = 1627\ m/s$. Fig.9 shows the detailed detonation structures after the shutdown of the hot jet. In Fig.9, almost only one relatively regular detonation cell can be observed in the channel, which is similar with experimental images of CJ detonation for the same $H_2/O_2/Ar$ mixture presented by Pintgen et al.[72].

A control calculation is set up in the straight channel without the cavity embedded as a comparison. In the control simulation, first, detonation initiation is realized successfully using a hot jet with a larger width of X_4 = 0.4 cm, and then the hot jet is shut down. After the shutdown of the hot jet, the hot jet influence gradually vanishes. In order to totally avoid the hot jet influence, only the dynamically stable

detonation is focused when the flow field has already undergone a long period evolution after the shutdown of the hot jet that the hot jet influence can be recognized totally vanished.

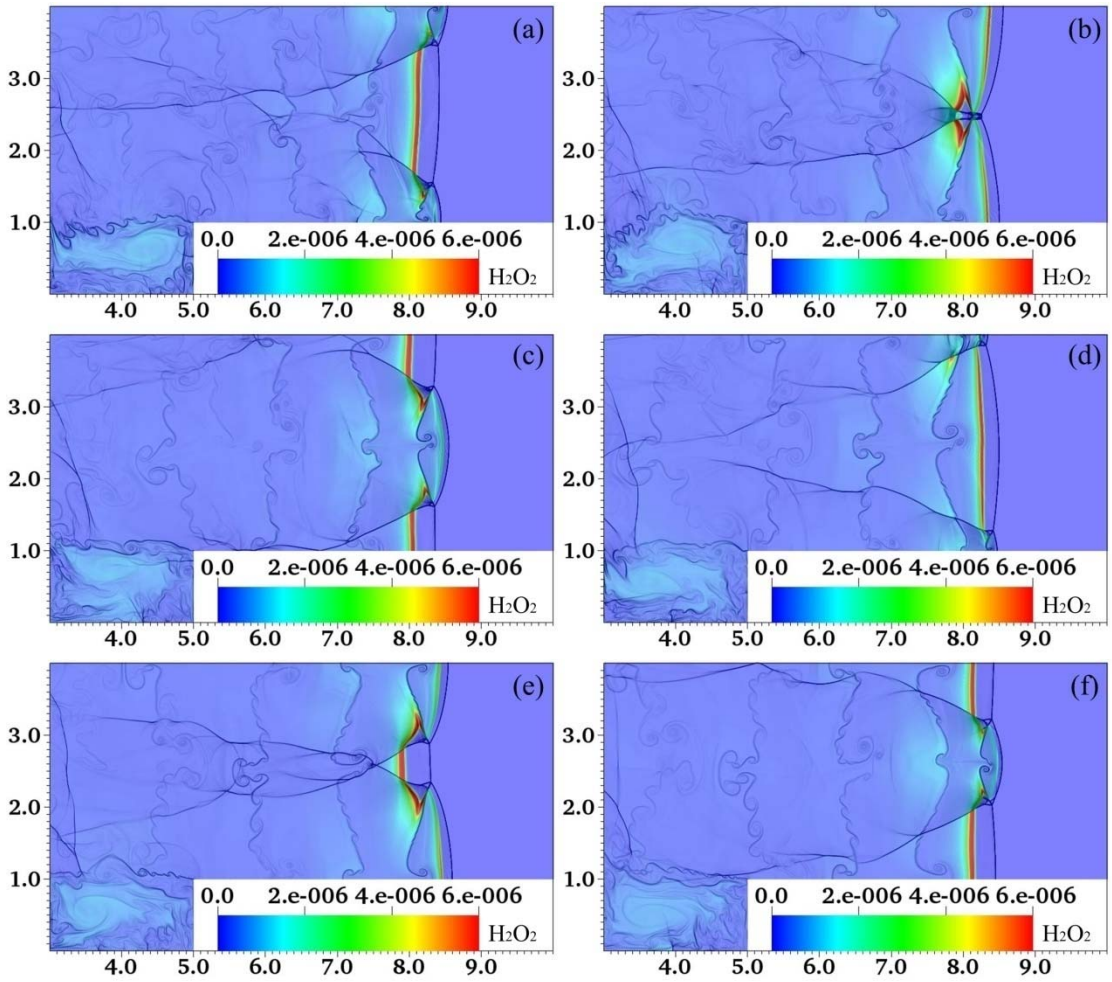

Fig.9 Density schlieren images and contours of H_2O_2 mass fractions for detonation propagation after the shutdown of the hot jet. (a) $t = 887.31\ \mu s$; (b) $t = 897.01\ \mu s$; (c) $t = 906.53\ \mu s$; (d) $t = 916.12\ \mu s$; (e) $t = 926.23\ \mu s$; (f) $t = 936.37\ \mu s$

Fig.10 shows the location history of detonation front in the control simulation. It is suggested that after about $t = 750\ \mu s$, an approximately straight line is formed. Therefore, the relative propagation velocity is obtained as $v_2 = -32.3\ m/s$, and hence the corresponding absolute propagation velocity is

$V_2 = v_2 + V_{CJ} = 1594.7\ \mathrm{m/s}$.

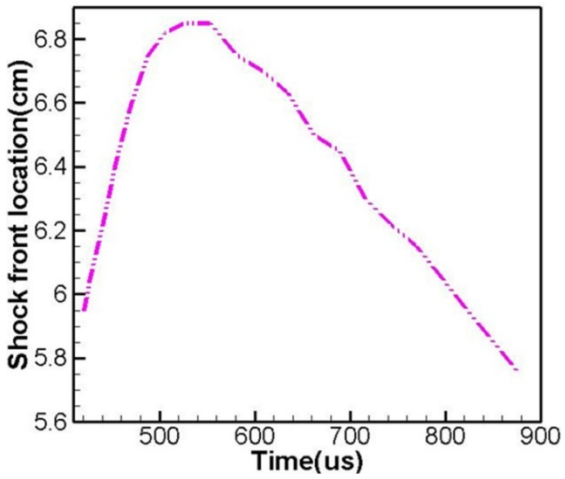

Fig.10 The location history of detonation front without the cavity embedded in the channel.

The hot jet is shut down at $t = 500\ \mu\mathrm{s}$.

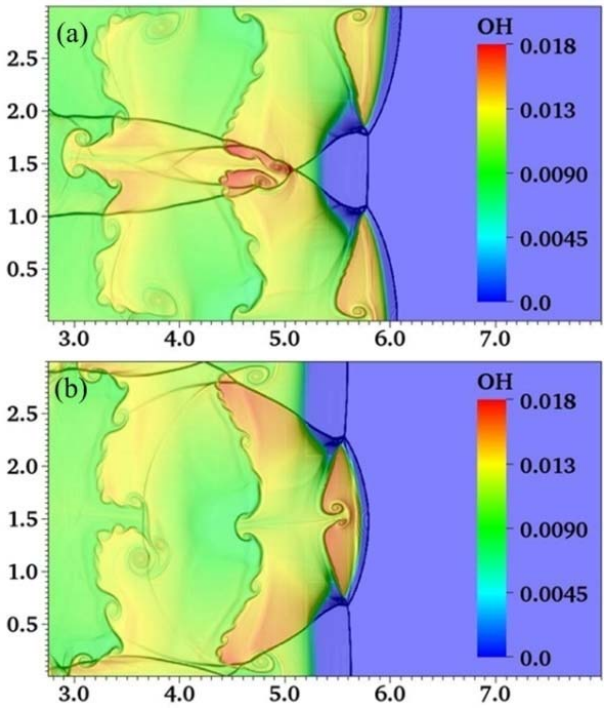

Fig.11 The CJ detonation after the shutdown of the hot jet without the cavity embedded in the channel. (a) $t = 818.44\ \mu\mathrm{s}$; (b) $t = 900\ \mu\mathrm{s}$.

It is reported that in a straight channel after the shutdown of the hot jet, a dynamically stable CJ detonation can be formed finally[21]. As shown in Fig.11, the

final stable CJ detonation is more similar to the experimental images of CJ detonation[72]. Compared with that in Fig.10, it is observed that detonation cells in Fig.11 are more symmetrical and regular. Table 2 lists the propagation velocities with and without the cavity embedded in the channel, respectively. It is shown that in the cavity-based channel the absolute propagation velocity is larger than that in the straight channel without the cavity embedded in the channel. If the case in the straight channel without the cavity embedded is regarded as a standard CJ detonation[21][22], then detonation in the cavity-based channel in Fig.9 is actually a slightly overdriven detonation after the shutdown of the hot jet, and the corresponding overdrive degree is obtained as $f = 1.041$ ($f = (\frac{V_1}{V_2})^2$).

Table 2 The relative and absolute velocities with and without the cavity embedded, respectively.

	With the cavity	**Without the cavity**
Relative velocity	$v_1 = 0$	$v_2 = -32.3$ m/s
Absolute velocity	$V_1 = 1627$ m/s	$V_2 = 1594.7$ m/s

In a straight channel without the cavity embedded, the hot jet plays an important role in the formation of overdriven detonation, and overdriven detonation gradually attenuates to the stable CJ detonation after the shutdown of the hot jet[21]. However, in a cavity-based channel, a slightly overdriven detonation is formed eventually after the shutdown of the hot jet, which indicates that the cavity also has some influence to accelerate detonation propagation in the supersonic combustible mixture.

Fig.12 shows the Mach contours and sonic lines in the cavity-based channel after the shutdown of the hot jet. The majority area between the front of the slightly

overdriven detonation and the right edge of the cavity is subsonic, and there exists a small subsonic channel in the vicinity of the right edge of the cavity in all the successive four frames which is marked by yellow circles. Therefore, it is indicated that the acoustic wave produced by pressure oscillations in the cavity can make an impact on detonation front after its crossing through the subsonic channel, thus finally resulting in the slightly overdriven detonation in the cavity-based channel.

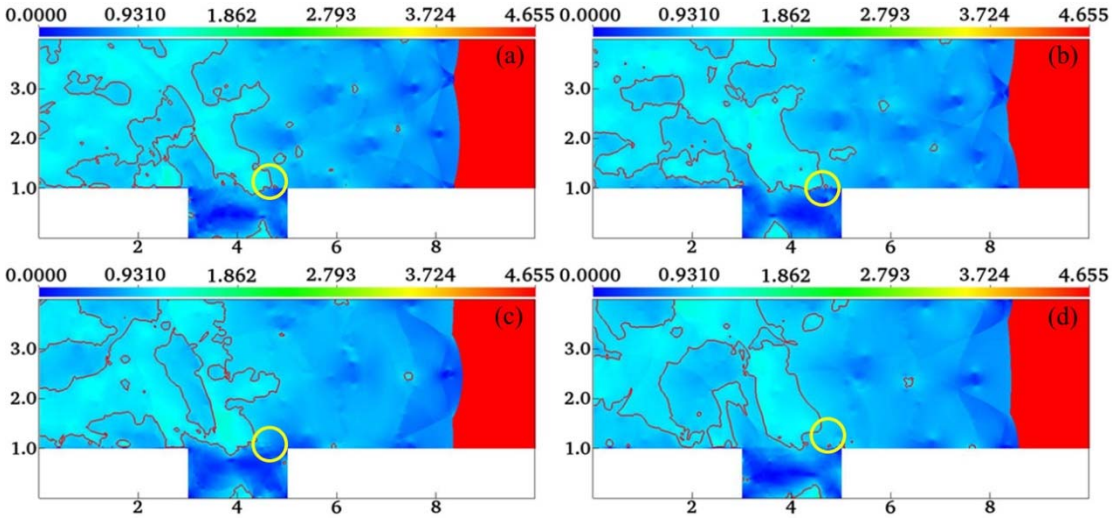

Fig.12 Mach contours and sonic lines after the shutdown of the hot jet in the cavity-based channel.

(a) $t = 496.11\ \mu s$; (b) $t = 631.51\ \mu s$; (c) $t = 801.61\ \mu s$; (d) $t = 944.84\ \mu s$.

4.3 Effects of cavity sizes

To provide an elementary understanding of the effects of cavity sizes on detonation combustion in supersonic combustible mixtures, a systemic of cavity-based detonation simulations are conducted, where the cavity width L and depth D are investigated independently while the other parameters are all kept the same. As previously discussed, the cavity can accelerate detonation initiation and propagation in the supersonic combustible mixture. Therefore, in order that the effects

of cavity sizes can be evaluated directly, the distances of detonation propagation in the supersonic combustible mixture for different cavity sizes are measured at the same given time $t = 700\ \mu s$ when detonation has already realized the constant-velocity propagation, which can be indicated in Fig.8.

4.3.1 Effects of cavity width

In Fig.13, five different cavities with widths varied from L = 2.0 cm to 4.0 cm are investigated while the cavity depth is kept the same as D = 1.0 cm. The locations of the detonation fronts in Fig.13(a)-(c) show a very slow increase, which are almost maintained in the same position of approximately X = 8.05 cm. However, in Fig.13(d)(e) the locations of the detonation fronts jump to about X = 8.9 cm, which presents an obvious difference from that in Fig.13(a)-(c). It is experimentally reported that under certain conditions for the flow over cavities, there exists a minimum cavity width below which no cavity oscillations occur[73]. For the given flow here, there should exist a minimum cavity width L_{min} between L = 3.0 cm in Fig.13(c) and L = 3.5 cm in Fig.13(d), that is $3.0\ \text{cm} \le L_{\min} \le 3.5\ \text{cm}$. When the width is below L_{min}, only some pressure wave oscillations in the cavity can make some relatively weak impacts on detonation initiation and propagation, but no cavity oscillations can occur. If the width reaches the critical value L_{min}, then cavity oscillations are generated which can significantly accelerate detonation initiation and propagation in the supersonic combustible mixture.

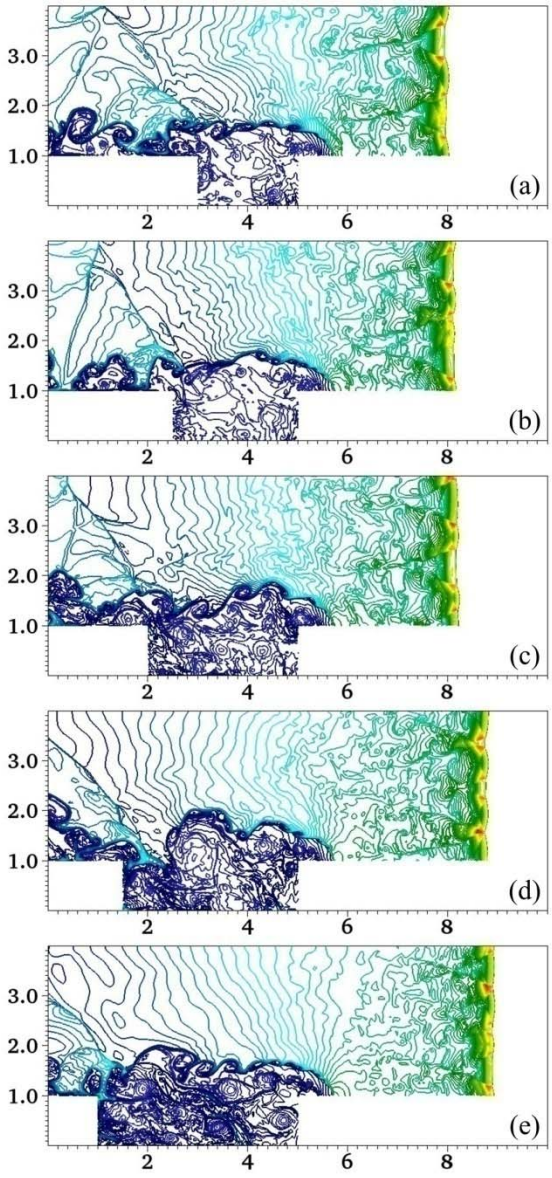

Fig.13 Detonation propagation for five different cavity widths at $t = 700\ \mu s$. (a) L = 2.0 cm; (b) L = 2.5 cm; (c) L = 3.0 cm; (d) L = 3.5 cm; (e) L = 4.0 cm.

4.3.2 Effects of cavity depth

Fig.14 shows five different cavities with depths varied from D = 1.0 cm to 3.0 cm while the cavity width is kept the same as L = 2.0 cm. The cavities in Fig.14(a)-(c) can be considered as shadow cavities while those in Fig.14(d)(e) can be considered as deep ones. In Fig.14(a)-(c) the locations of the detonation fronts almost are kept in the same position of about X = 8.05 cm. While compared with Fig.14(a)-(c), an obvious

location increase is observed in Fig.14(d)(e) where the location is approximately X = 8.5 cm. It is indicated that when the cavity is shadow, it does not make any more help for detonation initiation and propagation when purely increasing the cavity depth. Previous investigation[74] also reported that the cavity depth has little effect on cavity oscillations in shallow cavities, which is in close agreement with the current results obtained here. However, different from shadow cavities, deep cavities can act as resonators under certain flow conditions which can generate resonant oscillations[67]. When the cavity becomes a deep one, it can play an unnegligible role in detonation initiation and propagation in the supersonic combustible mixture due to resonant oscillations in the cavity.

The characteristics of cavities have been investigated numerously and cavity-based flameholders have been widely used in scramjet combustors. A detailed review of cavity researches is beyond the scope of this paper. However, through the investigation of the effects of cavity sizes, it is indicated that many mature theories involved in cavities can be directly applied for cavity-based detonation combustion in supersonic combustible mixtures, which can help lead a clear direction for further numerical and experimental investigations of cavity-based detonation combustion in supersonic combustible mixtures.

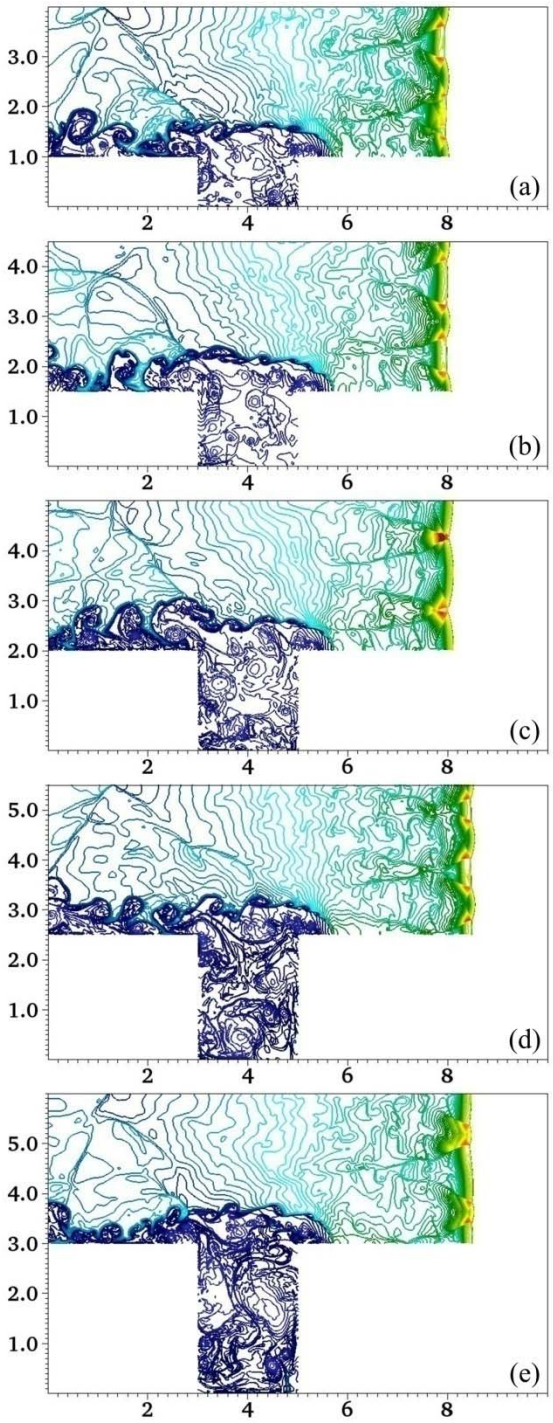

Fig.14 Detonation propagation for five different cavity depths at $t = 700\ \mu s$. (a) D = 1.0 cm; (b) D = 1.5 cm; (c) D = 2.0 cm; (d) D = 2.5 cm; (e) D = 3.0 cm.

5 Conclusion

To investigate detonation combustion using a hot jet initiation in cavity-based

channels filled with the supersonic hydrogen-oxygen mixture, two-dimensional reactive Euler equations with a detailed reaction model are solved numerically using the adaptive mesh refinement method. The major results of the present work are as follows

1. The comparison between simulations in cavity-based channels and straight channels without the cavity embedded indicates that the cavity can help realize detonation initiation in the supersonic combustible mixture using a hot jet. The pressure wave resulting from the subsonic combustion in the cavity can enhance the strength of the bow shock induced by the hot jet through pressure oscillations, thus leading to the formation of Mach reflection on the upper wall which is critical for the successful initiation. It is indicated that detonation initiation can be realized even using a weaker hot jet in cavity-based channels filled with supersonic combustible mixtures compared with that in straight channels without a cavity embedded.
2. The cavity also has an important influence on detonation propagation in the supersonic combustible mixture. After the shutdown of the hot jet, the acoustic wave produced by the subsonic combustion in the cavity can accelerate detonation propagation after crossing through the subsonic channel in the vicinity of the right edge of the cavity, thus resulting in a slightly overdriven detonation.
3. For a given flow with a shadow cavity embedded, there should exist a minimum cavity width L_{min}. When the width is below L_{min}, only some

pressure wave oscillations in the cavity can make some impacts on detonation initiation and propagation, but no cavity oscillations can occur. When the width reaches the critical value L_{min}, cavity oscillations are generated which can significantly accelerate detonation initiation and propagation in the supersonic combustible mixture.

4. For a shadow cavity, it does not make any more help for detonation initiation and propagation when purely increasing the cavity depth. However, when the cavity becomes a deep one, it can play an unnegligible role in accelerating detonation initiation and propagation in the supersonic combustible mixture due to resonant oscillations occurred in the cavity.

6 Acknowledgements

This work is supported by National Natural Science Foundation of China under Grant No. 91441201, Innovative Sustentation Fund for Excellent Ph.D. Students in NUDT under Grant No. B140101 and Chinese Scholarship Council (CSC) under Grant No. 201403170401.

Reference

[1] Kailasanath K. Review of propulsion applications of detonation waves. AIAA J 2000;38:1698-708.

[2] Smirnov NN, Nikitin VF. Modeling and simulation of hydrogen combustion in engines. Int J Hydrogen Energy 2014;39:1122-36.

[3] Smirnov NN, Betelin VB, Shagaliev RM, Nikitin VF, Belyakov IM, Deryuguin YN, Aksenovb SV, Korchazhkin DA. Hydrogen fuel rocket engines simulation using LOGOS code. Int J Hydrogen Energy 2014;39:10748-56.

[4] Smirnov NN, Nikitin VF, Stamov LI, Altoukhov DI. Supercomputing simulations of detonation of hydrogen-air mixtures. Int J Hydrogen Energy 2015;40:11059-74.

[5] Zhang B, Kamenskihs V, Ng HD, Lee JHS. Direct blast initiation of spherical gaseous detonations in highly argon diluted mixtures. Proc Combust Inst 2011;33:2265-71.

[6] Zhang B, Ng HD, Mével R, Lee JHS. Critical energy for direct initiation of spherical detonations in H_2/N_2O/Ar mixtures. Int J Hydrogen Energy 2011;36:5707-16.

[7] Zhang B, Ng HD, Lee JHS. Measurement of effective blast energy for direct initiation of spherical gaseous detonations from high-voltage spark discharge. Shock Waves 2012;22:1-7.

[8] Knystautas R, Lee JHS, Moen I, Wagner HGG. Direct initiation of spherical detonation by a hot turbulent gas jet. Seventeenth Symposium (International) on Combustion 1979;17:1235-1245.

[9] Carnasciali F, Lee JHS, Knystautas R, Fineschi F. Turbulent jet initiation of detonation. Combust Flame 1991;84:170-80.

[10] Liu SJ, Lin ZY, Liu WD, Lin W, Zhuang FC. Experimental realization of H_2/Air continuous rotating detonation in a cylindrical combustor. Combust Sci Technol 2012;184:1302-17.

[11] Iglesias I, Vera M, Sánchez AL, Liñán A. Numerical analyses of deflagration initiation by a hot jet. Combust Theor Model 2012; 16: 994-1010.

[12] Carpio J, Iglesias I, Vera M, Sánchez AL, Liñán A. Critical radius for hot-jet ignition of hydrogen-air mixtures. Int J Hydrogen Energy 2013;38:3105-09.

[13] Ishii K, Kataoka H, Kojima T. Initiation and propagation of detonation waves in combustible high speed flows. Proc Combust Inst 2009;32:2323-30.

[14] Han X, Zhou J, Lin ZY. Experimental investigations of detonation initiation by hot jets in supersonic premixed flows. Chin Phys B 2012;21:124702.

[15] Han X, Zhou J, Lin ZY, Liu Y. Deflagration-to-Detonation transition induced by hot jets in a supersonic premixed airstream. Chin Phys Lett 2013;30:054701.

[16] Jackson SI, Shepherd JE. Detonation initiation in a tube via imploding toroidal shock waves. AIAA J 2008;46:2357-67.

[17] Melguizo-Gavilanes J, Bauwens L. Shock initiated ignition for hydrogen mixtures of different concentrations. Int J Hydrogen Energy 2013;38:8061-67.

[18] Melguizo-Gavilanes J, Rezaeyan N, Tian M, Bauwens L. Shock-induced ignition with single step Arrhenius kinetics. Int J Hydrogen Energy 2011;36:2374-80.

[19] Driscoll R, Stoddard W, George AS, Gutmark EJ. Shock transfer and shock-initiated detonation in a dual pulse detonation engine/crossover system. AIAA J 2015;53:132-39.

[20] Driscoll R, George AS, Stoddard W, Munday D, Gutmark EJ. Characterization of shock wave transfer in a pulse detonation engine-crossover system. AIAA J 2015.

[21] Cai XD, Liang JH, Lin ZY, Deiterding R, Qin H, Han X. Adaptive mesh refinement–based numerical simulation of detonation initiation in supersonic combustible mixtures using a hot jet. ASCE J Aerosp Eng 2015;28:04014046.

[22] Cai XD, Liang JH, Lin ZY, Deiterding R, Liu Y. Parametric study of detonation initiation using a hot jet in supersonic combustible mixtures. Aerosp Sci Tech 2014;39:442-55.

[23] Cai XD, Liang JH, Lin ZY, Deiterding R, Zhuang FC. Detonation initiation and propagation

in nonuniform supersonic combustible mixtures. Combust Sci Tech 2015;187:525-536.

[24] Cai XD, Liang JH, Deiterding R, Che YG, Lin ZY. Adaptive mesh refinement based simulations of three-dimensional detonation combustion in supersonic combustible mixtures with a detailed reaction model. Int J Hydrogen Energy 2015.

[25] Cai XD, Liang JH, Deiterding R, Lin ZY. Numerical simulation of detonation initiation and propagation in supersonic combustible mixtures with non-uniform species. AIAA J 2016.

[26] Liang JH, Cai XD, Lin ZY, Deiterding R. Effects of a hot jet on detonation initiation and propagation in supersonic combustible mixtures. Acta Astronaut 2014;105:265-77.

[27] Berger M, Oliger J. Adaptive mesh refinement for hyperbolic partial differential equations. J Comput Phys 1984;53:484-512.

[28] Deiterding R. Parallel adaptive simulation of multi-dimensional detonation structures [Ph.D. thesis]. Cottbus, Brandenburg: Brandenburg University of Technology; 2003.

[29] Liang Z, Browne S, Deiterding R, Shepherd JE. Detonation front structure and the competition for radicals. Proc Combust Inst 2007;31:2445-53.

[30] Deiterding R. A parallel adaptive method for simulating shock-induced combustion with detailed chemical kinetics in complex domains. Comput Struct 2009;87:769-83.

[31] Deiterding R. High-Resolution numerical simulation and analysis of Mach reflection structures in detonation waves in low-pressure H_2-O_2-Ar mixtures: A summary of results obtained with the adaptive mesh refinement framework AMROC. J combust 2011;2011.

[32] Ziegler JL, Deiterding R, Shepherd JE, Pullin DI. An adaptive high-order hybrid scheme for compressive, viscous flows with detailed chemistry. J Comput Phys 2011;230:7598-630.

[33] Westbrook CK. Chemical kinetics of hydrocarbon oxidation in gaseous detonations. Combust

Flame 1982;46:191-210.

[34] Handa T, Miyachi H, Kakuno H, Ozaki T, Maruyama S. Modeling of a feedback mechanism in supersonic deep-cavity Flows. AIAA J 2015;53:420-25.

[35] Li WP, Nonomura T, Oyama A, Fujii K. Feedback mechanism in supersonic laminar cavity flows. AIAA J 2013;51:253-57.

[36] Schmit RF, Grove JE, Semmelmayer F, Haverkamp M. Nonlinear feedback mechanisms inside a rectangular cavity. AIAA J 2014;52:2127-42.

[37] Yeom HW, Seo BG, Sung HG. Numerical analysis of a scramjet engine with intake sidewalls and cavity flameholder. AIAA J2013;51:1566-75.

[38] Tatman BJ, Rockwell RD, Goyne CP, McDaniel JC, Donohue JM. Experimental study of vitiation effects on flameholding in a cavity flameholder. J Propul Power 2013;29:417-23.

[39] Yeom HW, Seo BG, Sung HG. Numerical analysis of a scramjet engine with intake sidewalls and cavity flameholder. AIAA J 2013;51:1566-75.

[40] Kang SH, Lee YJ, Yang SS, Smart MK, Suraweera MK. Cowl and cavity effects on mixing and combustion in scramjet engines. J Propul Power 2011;27:1169-77.

[41] Mahmoudi Y, Mazaheri K. High resolution numerical simulation of the structure of 2-D gaseous detonations. Proc Combust Inst 2011;33:2187-94.

[42] Radulescu MI, Lee JHS. The failure mechanism of gaseous detonations: experiments in porous wall tubes. Combust Flame 2002;131:29-46.

[43] Radulescu MI, Sharpe GJ, Lee JHS, Kiyanda CB, Higgins AJ, Hanson RK. The ignition mechanism in irregular structure gaseous detonations. Proc Combust Inst 2005;30:1859-67.

[44] Shepherd JE. Detonation in gases. Proc Combust Inst 2009;32:83-98.

[45] Radulescu MI, Sharpe GJ, Law CK, Lee JHS. The hydrodynamic structure of unstable cellular detonations. J Fluid Mech 2007;580:31-81.

[46] Gamezo VN, Desbordes D. Oran ES. Formation and evolution of two-dimensional cellular detonations. Combust Flame 1999;116:154-65.

[47] Sharpe GJ, Falle SAE. Two-dimensional numerical simulations of idealized detonations. Proc R Soc Lond A 2000;456:2081-2100.

[48] Mach P, Radulescu MI. Mach reflection bifurcations as a mechanism of cell multiplication in gaseous detonations. Proc Combust Inst 2010;33:2279-85.

[49] Hu XY, Khoo BC, Zhang DL, Jiang ZL. The cellular structure of a two-dimensional H_2/O_2/Ar detonation wave. Combust Theory Model 2004;8:339-59.

[50] Hu XY, Zhang DL, Khoo BC, Jiang ZL. The structure and evolution of a two-dimensional H_2/O_2/Ar cellular detonation. Shock Waves 2005;14:37-44.

[51] Mahmoudi Y, Mazaheri K. Triple point collision and hot spots in detonations with regular structure. Combust Sci Tech 2012;184:1135-51.

[52] Mével R, Davidenko D, Austin JM, Pintgen F, Shepherd JE. Application of a laser induced fluorescence model to the numerical simulation of detonation waves in hydrogen-oxygen-diluent mixtures. Int J Hydrogen Energy 2014;39:6044-60.

[53] Strehlow RA. Gas phase detonations: Recent developments. Combust Flame 1968;12:81-101.

[54] Goodwin D. Tech. Rep. California Institute of Technology, http://www.cantera.org.

[55] Leer BV. On the relation between the upwind-differencing schemes of Godunov, Engquist-Osher and Roe. SIAM J Sci Statist Comput 1984;5:1-20.

[56] Sharpe GJ. Transverse waves in numerical simulations of cellular detonations. J Fluid Mech

2001;447:31-51.

[57] Smirnov NN, Betelin VB, Nikitin VF, Stamov LI, Altoukhov DI. Accumulation of errors in numerical simulations of chemically reacting gas dynamics. Acta Astronaut 2015;117: 338-55.

[58] Samtaney R, Pullin DI. On initial-value and self-similar solutions of the compressible Euler equations. Phys Fluids 1996;8:2650-55.

[59] Oran E.S., Jr JWW, Stefaniw EI, Lefebvre MH, Jr JDA. A numerical study of a two-dimensional H_2-O_2-Ar detonation using a detailed chemical reaction model. Combust Flame 1998;113:147-63.

[60] Mazaheri K, Mahmoudi Y, Sabzpooshani M, Radulescu MI. Experimental and numerical investigation of propagation mechanism of gaseous detonations in channels with porous walls. Combust Flame 2015;162:2638-59.

[61] Mahmoudi Y, Mazaheri K. High resolution numerical simulation of triple point collision and origin of unburned gas pockets in turbulent detonations. Acta Astronaut 2015;115:40-51.

[62] Emami S, Mazaheri K, Shamooni A, Mahmoudi Y. LES of flame acceleration and DDT in hydrogen-air mixture using artificially thickened flame approach and detailed chemical kinetics. Int J Hydrogen Energy 2015;40:7395-408.

[63] Maxwell BM, Tawagi P, Radulescu MI. The role of instabilities on ignition of unsteady hydrogen jets flowing into an oxidizer. Int J Hydrogen Energy 2013;38:2908-18.

[64] Mazaheri K, Mahmoudi Y, Radulescu MI. Diffusion and hydrodynamic instabilities in gaseous detonations. Combust Flame 2012;113:2138-54.

[65] Mahmoudi Y, Mazaherin K, Parvar S. Hydrodynamic instabilities and transverse waves in

propagation mechanism of gaseous detonations. Acta Astronaut 2013;91:263-82.

[66] Mahmoudi Y, Karimi N, Deiterding, Emami S. Hydrodynamic instabilities in gaseous detonations: Comparison of Euler, Navier–Stokes, and Large-Eddy simulation. J Propul Power 2014;30:384-96.

[67] East LF. Aerodynamic induced resonance in rectangular cavities. J Sound Vibrations 1966;3:277-87.

[68] Deiterding R, Bader G. High-resolution simulation of detonations with detailed chemistry. Analysis and Numerics for Conservation Laws 2005;2005:69-91.

[69] Smirnov NN, Nikitin VF, Alyari-Shourekhdeli Sh. Transitional regimes of wave propagation in metastable systems. Combust Explos Shock Waves 2008;44(5):517-28.

[70] Smirnov NN, Nikitin VF, Phylippov YuG. Deflagration to detonation transition in gases in tubes with cavities. J Eng Phys Thermophys 2010;83(6):1287-316.

[71] Li C, Kailasanath K. Detonation initiation by annular-jet-induced imploding shocks. J Propul Power 2005;21.

[72] Pintgen F, Eckett CA, Austin JM, Shepherd JE. Direct observations of reaction zone structure in propagating detonations. Combust Flame 2003;133:211-29.

[73] Karamcheti K. Sound radiated from surface cutouts in high-speed flows [Ph.D. thesis]. California: California Institute of Technology; 1956.

[74] Sarohiav V. Experimental investigation of oscillations in flows over shallow cavities. AIAA J 1977;15:984-91.